

28. $^{40}\text{Ar}/^{39}\text{Ar}$ DATING OF GABBROS FROM THE OCEAN/CONTINENT TRANSITION OF THE WESTERN IBERIA MARGIN: PRELIMINARY RESULTS¹

Gilbert Féraud,² Marie-Odile Beslier,³ Guy Cornen⁴

Abstract

$^{40}\text{Ar}/^{39}\text{Ar}$ analyses were performed on two bulk samples of plagioclase extracted from flaser gabbros that constitute the entire basement core at Site 900. The two age spectra are disturbed by alteration processes and possibly excess argon. One of the two plagioclases, despite a strong contamination by K-rich phases, displays a flat section of apparent ages on its age spectrum with a weighted mean of 136.4 ± 0.3 m.y., which may represent a reasonable estimate of the closure time of the plagioclase. Considering the petro-structural constraints on the evolution of these gabbros (Cornen et al., chapter 26, this volume), this age is coherent with the final stage of the metamorphic event that affected these gabbros at the end of the Mesozoic continental rifting. When compared to the previous $^{40}\text{Ar}/^{39}\text{Ar}$ plateau-ages obtained on magmatic rocks of the Galicia Margin to the north and Goringe Bank to the south, this age is consistent with a northward propagation of the Atlantic ocean opening.

INTRODUCTION

The main objective of Leg 149 was to determine the structure and the nature of the ocean-continent transition (OCT) of the western Iberia passive continental margin in the Iberia Abyssal Plain (IAP). The basement was reached at three sites where structural highs of the basement are buried under a 650-690-m thick sedimentary cover of Pleistocene to Barremian age. At Site 897 (Fig. 1), peridotites were drilled on a basement high which is the southward prolongation of the peridotite ridge of the Galicia Margin (Beslier et al., 1993; Whitmarsh et al., 1993). At Site 899B, the acoustic basement consists mainly of ultramafic breccias. Gabbros were recovered eastward at Site 900, where continental basement was expected (Shipboard Scientific Party, 1993). Petro-structural studies of these rocks show that the evolution of the peridotite is compatible with an uplift beneath a rift zone (Beslier et al., this volume; Cornen et al., chapter 26, this volume), and that the gabbros were dynamically recrystallized during an intense shear deformation event. Time constraints are essential to determine the evolution of these rocks, which provide information about the processes of lithospheric break-up and/or very first oceanic accretion stages. According to studies of the peridotites previously drilled and sampled with the submersible *Nautilus* on the northward adjacent Galicia Margin, the emplacement of the mantle rocks near the seafloor occurred at the end of the continental rifting (Boillot et al., 1988; 1989; Féraud et al., 1988; Girardeau et al., 1988).

Here we present the first results of $^{40}\text{Ar}/^{39}\text{Ar}$ dating of plagioclase from two samples of sheared gabbro drilled at Site 900.

GEOLOGICAL SETTING AND SAMPLE DESCRIPTION

Site 900 is located 75 km east of Site 897 where the basement of the OCT is made of mantle rocks, and 45 km west of Site 901 located

¹Whitmarsh, R.B., Sawyer, D.S., Klaus, A., and Masson, D.G. (Eds.), 1996. *Proc. ODP, Sci. Results*, 149: College Station, TX (Ocean Drilling Program).

²Institut de Géodynamique, URA CNRS 1279, Université de Nice Sophia-Antipolis, 06108 Nice cedex 2, France, ferlaud@mimosas.unice.fr

³Laboratoire de Géodynamique sous-marine, Université Paris 6, BP48, 06230 Villefranche sur Mer, France.

⁴Laboratoire de Pétrologie Structurale, 2 rue de la Houssinière, 44072 Nantes cedex 03, France.

on a large tilted block of the margin presumably made of continental crust (Shipboard Scientific Party, 1993, fig. 1). At Site 900, a total of 56.1 m of basement was drilled and 27.7 m of material was recovered. The basement consists mainly of fine-grained gabbros which are locally highly fractured and brecciated. A detailed description of the cores is given by Sawyer, Whitmarsh, Klaus, et al. (1994) and Cornen et al. (chapter 26, this volume). Only the main characteristics of the series are given here.

The gabbros appear to be mainly homogeneous fine-grained rocks, grading downcore from greenish-white to a grayish-green and brownish color. They locally display a clear foliation marked by alternating mafic and felsic bands (e.g., Section 83R-2). In such intervals, the rocks show a typical structure of flaser gabbros with porphyroclasts rotated and aligned along the foliation plane. The development of C-S features attests to shear deformation of the rocks. Although less obvious, the same foliation characterizes the fine-grained dark intervals, in bands less than 1 mm thick. The coarse-banded intervals are distributed over the whole thickness of the drilled section. The transition between the fine-grained dark facies and the coarser banded facies is often overprinted by the late fracturing. In some sections however, this transition is clearly primary, as the coarser banded intervals grade rapidly over a few millimeters into finer-banded zones (e.g., Sample 149-900A-82R-1, 70-85 cm).

The two samples selected for preliminary dating are representative of these two main facies. Sample 149-900A-83R-2, 77-82 cm (labeled here 83R77-82) is located in the thickest coarse-banded interval recovered in the cores (interval 149-900A-83R-2, 45-110 cm). Sample 149-900A-85R-5, 18-23 cm (labeled here 85R18-23), recovered 16m below, is representative of the fine-grained facies.

Throughout the whole drilled series, the primary mineralogy is composed of clinopyroxene, plagioclase, and a few oxides as accessories. A secondary paragenesis developed as amphibole, chlorite, epidote, and locally, sericite.

In thin section, the texture of the gabbros is granuloblastic to porphyroclastic. In sample 83R77-82, 5% to 10% of porphyroclasts of both pyroxene and plagioclase are embedded in a groundmass of small-sized equant neoblasts (0.2 mm) of the same minerals (Fig. 2). The foliation is well-marked by alternating beds (a few mm thick) of pyroxene and grain boundary plagioclase neoblasts, which exhibit frequent triple junctions. In the plagioclase bands, this mosaic texture is locally underlined by thin rims of chlorite at grain boundaries, and sericite patches are observed in or at the periphery of plagioclase crystals. The proportion of sericite is low (estimated at less than 1%

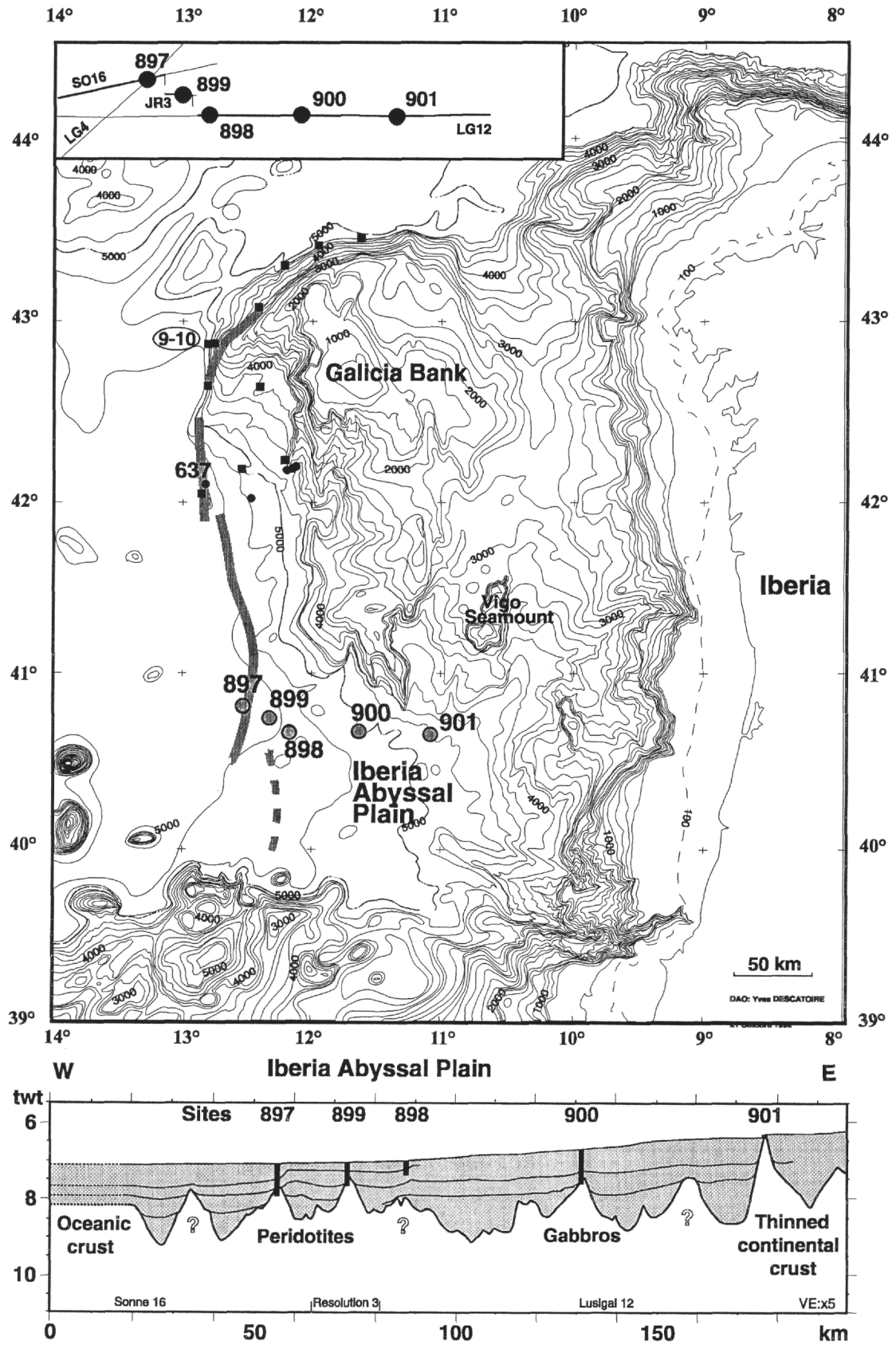


Figure 1. Bathymetric map of western Iberia Margin (Lallemand et al., 1985) and schematic cross-section through the Iberia Abyssal Plain showing the location of sites drilled during Leg 149. Former drill sites (Leg 103: small black dots), and dive sites (*Galnaute* cruise: black squares, including dive sites 9-10), on the Galicia Margin are also located. The gray dashed line indicates the peridotite ridge.

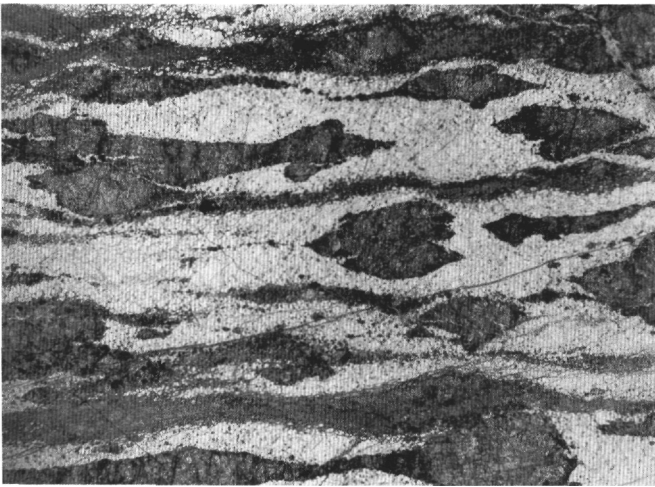


Figure 2. Photomicrograph of Sample 83R77-82 showing porphyroclastic texture and well-marked foliation (see text for details).

in volume) and plagioclase appears dominantly fresh. Both plagioclase porphyroclasts (which are elongated in the foliation), and neoblasts display mechanical twins and undulating extinctions. Green spinel, approximately 100 to 150 μm in size, occurs in places in the plagioclase neoblasts. Pyroxene porphyroclasts are also preserved in pyroxene neoblast lenses and bands. They are up to 6 mm in size and display thin exsolution lamellae which are locally bent. Pyroxene is partially retrometamorphosed to fibrous amphibole, which locally forms continuous bands in the foliation.

The texture of sample 85R18-23 is granuloblastic. Except for the absence of porphyroclasts, the texture and primary mineralogy of this sample is comparable to that of sample 83R77-82. The same alternation of plagioclase and pyroxene neoblast bands defines the foliation. Although the bands are thinner than in the previous sample (1-2 mm), the size of the neoblasts is comparable (0.2 mm). Apparently, no spinel is preserved. Secondary mineralogy includes chlorite-rimming plagioclase neoblasts, amphibole as a replacement for clinopyroxene (although to a lesser extent than in sample 83R77-82), and actinolite and epidote as fracture fillings. Secondary mineralogy differs from the previous sample by the absence of sericite and by the noticeable occurrence of albitic framework inside plagioclase neoblasts.

Such textures clearly result from dynamic recrystallization of the gabbros during intense shear deformation. Experimental data on silicates (olivine, quartz and pyroxene) show that during plastic deformation under steady state conditions, the grain size produced by dynamic recrystallization depends on the applied deviatoric stress (e.g., Mercier et al., 1977). No experimental data are available for plagioclase. However, the similar size of the neoblasts in the two samples strongly suggests that the variations in the thickness of bands do not result from varying degrees of deformation, but rather represent an initial heterogeneity of the gabbros. Textural relationships show also that the retrometamorphism to greenschist facies conditions is static and clearly occurs after the dynamic recrystallization of the rock.

Phase Composition

Phase compositions have been obtained through a CAMEBAX (SX50) microprobe (Microprobe Ouest, Brest, analytical details are given by Cornen et al., chapter 26, this volume). Selected data are listed in Table 1.

Pyroxene porphyroclasts and neoblasts are all diopside that displays a slight evolution toward augite ($\text{Wo}_{48.8}\text{En}_{42.9}\text{Fs}_{8.3}$ to $\text{Wo}_{35.1}\text{En}_{48.6}\text{Fs}_{16.3}$). Their crystallization under higher pressures than

pyroxenes from gabbros recovered in presumably comparable settings, that is, slow-spreading ridges (Helmstaedt and Allen, 1977; Honnorez et al. 1984; Bonatti and Seyler, 1987; Bloomer et al., 1989), has been proposed by Cornen et al. (chapter 26, this volume) on the basis of their noticeably higher content of CaO , Al_2O_3 and Na_2O . The discrete presence of aluminous spinel with low Cr content (pleonaste) inside plagioclase neoblasts would have the same significance.

In sample 83R77-82, feldspars range from $\text{Or}_{0.4}\text{Ab}_{35.6}\text{An}_{64}$ in the porphyroclast core to $\text{Or}_{0.9}\text{Ab}_{42.5}\text{An}_{56.5}$ in the neoblasts without a compositional gap. The average Or content of 0.8% (values range from 0.3% to 1.2%) corresponds to a K_2O content between 0.058 wt% and 0.219 wt%. A slight difference appears between the neoblasts and the porphyroclast core which is more anorthitic and less potassic. In sample 85R18-23, which is devoid of porphyroclasts, neoblasts have a composition close to that of the previous sample: $\text{Or}_{0.5}\text{Ab}_{29.4}\text{An}_{70}\text{Or}_{0.5}\text{Ab}_{47.4}\text{An}_{53}$ with an Or content centered on 0.8% (0.4% to 1.2%).

The major difference between the two samples is the existence in the fine-grained sample (85R18-23) of neoblasts with an albitic framework with a composition centered on $\text{Or}_{0.4}\text{Ab}_{88.2}\text{An}_{11.4}$. In these albitic zones the K_2O content is lower, with a range of 0.02% to 0.06% K_2O by weight. In the coarse-banded sample (83R77-82), patches of sericite flakes (muscovite) occur, and albite is not apparent. Aside from the high K_2O content of sericite (between 8% and 10% by weight; Table 1), microprobe analyses show the existence of Ca and Mg, which is most likely due to contamination by the surrounding plagioclase and chlorite, probably because of the small size of the sericite flakes.

This secondary mineralogy (which includes actinolite to actinolitic hornblende replacing pyroxenes, chlorite, epidote, albite and sericite) is typically that of greenschist grade metamorphism which overprints and postdates the main shearing event.

$^{40}\text{Ar}/^{39}\text{Ar}$ AR RESULTS

Twenty-five mg of plagioclase (160-200 μm) were separated by a magnetic separator and then hand-picked under a microscope to select only the most transparent grains for analysis. The samples were irradiated for 70 hr in the McMaster reactor (Hamilton, Canada) with a total flux of 9×10^{18} n/cm². We piled up the samples and monitors along the axis of the irradiation canister. Eleven standard Hb₃Gr hornblendes (1072 Ma) were included in the 90-mm-long sample pile (Table 2).

In spite of a total flux gradient of 4% from the bottom to the top of the canister, the neutron flux received by each sample was known to within $\pm 0.2\%$. The analytical procedure was as described by Féraud et al. (1986). All errors in apparent ages and total ages are quoted at the 1 σ level and do not include the errors in the $^{40}\text{Ar}^*/^{39}\text{Ar}_K$ ratio and age of the monitor. The error in the $^{40}\text{Ar}^*/^{39}\text{Ar}_K$ ratio of the monitor is included in the "plateau age" error bar calculation.

From low to high temperature steps, both age spectra (Fig. 3) are characterized by a decrease of apparent ages (from 500° to 760°C), followed by a sharp increase in age, giving a flat section of over 72% (sample 83R77-82) and 44% (sample 85R18-23) of ^{39}Ar released, respectively. Then the high temperature ages increase regularly.

The very disturbed apparent ages displayed at low temperature correspond to very variable and increasing $^{37}\text{Ar}_{Ca}/^{39}\text{Ar}_K$ ratios probably indicating the degassing of K-rich secondary phases included in the plagioclase (as observed under the microscope). Another phenomenon which may affect these low temperature ages is excess ^{40}Ar , as suggested by both the increasing ages at high temperature (up to 148 and 160 m.y. for samples 83R77-82 and 85R18-23, respectively), and, more clearly, by the high apparent ages (up to 180 m.y.) obtained at low temperature on sample 85R18-23. The classical U-shaped age spectra commonly displayed by plagioclases affected by

Table 1. Selected analyses of plagioclase* 83R77-82 (number 1 to 4) and 85R18-23 (number 5 to 8) and muscovite 83R77-82 (number 9) of the dated samples.

Elements	83R77-82				85R18-23				83R77-82
	1 Pc	2 Pm	3 Nc	4 Nm	5 Nc	6 Nm	7 N	8 N	9
SiO ₂	52.843	52.385	54.225	52.787	50.840	52.212	55.226	65.809	46.692
TiO ₂	0.010	0	0	0	0.053	0	0	0.007	0.023
Al ₂ O ₃	29.700	30.055	29.192	29.785	31.317	30.163	28.791	21.728	36.113
Fe ₂ O ₃	0	0.051	0.117	0.169	0.120	0.162	0.122	0.219	0.022
MgO	0.007	0	0	0.005	0.002	0.017	0	0	0.521
CaO	12.783	13.350	11.857	12.408	14.904	13.566	11.076	2.713	0
Na ₂ O	4.389	4.176	4.888	4.758	3.360	4.083	5.563	10.564	1.207
K ₂ O	0.099	0.058	0.219	0.119	0.139	0.102	0.083	0.020	0.707
Total	99.830	100.075	100.497	100.031	100.736	100.304	100.861	101.060	10.100
Or	0.006	0.003	0.012	0.007	0.008	0.006	0.005	0.001	0.004
Ab	0.381	0.360	0.422	0.407	0.288	0.351	0.474	0.875	0.004
An	0.613	0.636	0.566	0.586	0.705	0.644	0.521	0.124	94.462

Notes: P = porphyroclast, N = neoblast, c = core, m = margin; Or, Ab, An = main molar components of feldspar.

Table 2. ⁴⁰Ar/³⁹Ar analytical data obtained on the plagioclases 83R77-82 and 85R18-23.

Temp °C	⁴⁰ Ar _{Atm} (%)	³⁹ Ar _K (%)	³⁷ Ar _{Ca} / ³⁹ Ar _K	⁴⁰ Ar*/ ³⁹ Ar _K	Age (Ma)
Sample 83R77-82					
500	63.69	3.59	1.289	5.203	147.4 ± 2.2
600	34.12	5.56	2.132	4.589	130.6 ± 1.2
700	54.63	5.56	5.053	4.272	121.9 ± 1.7
760	71.54	3.73	7.613	4.271	121.9 ± 2.1
820	23.76	4.04	10.083	4.778	135.9 ± 1.2
880	19.50	5.03	10.830	4.886	138.8 ± 1.2
930	22.43	5.20	11.968	4.790	136.1 ± 1.3
980	15.98	7.76	12.187	4.837	137.4 ± 1.1
1030	14.36	10.72	8.496	4.831	137.3 ± 0.8
1080	15.97	12.51	6.542	4.764	135.4 ± 0.7
1130	16.70	10.95	7.915	4.732	134.5 ± 0.8
1180	17.53	10.30	10.351	4.783	135.9 ± 1.0
1230	30.53	5.362	2.149	4.860	138.1 ± 1.7
1280	41.49	4.093	3.905	4.965	140.9 ± 2.4
1350	51.17	2.75	37.402	5.224	148.0 ± 3.2
Fuse	88.77	2.85	33.001	5.236	148.3 ± 7.5
					Total age = 135.9 ± 0.4
Sample 85R18-23					
500	80.31	4.14	2.140	6.414	180.0 ± 7.8
600	53.11	6.22	3.331	5.146	145.9 ± 2.3
700	79.04	5.28	7.197	3.607	103.5 ± 3.8
760	88.64	4.16	10.259	3.049	87.8 ± 6.2
820	43.74	4.31	18.454	4.196	119.8 ± 4.7
880	36.48	5.22	23.217	4.340	123.8 ± 3.6
930	36.75	6.95	27.393	4.378	124.8 ± 2.9
980	30.34	7.41	30.053	4.464	127.2 ± 3.0
1030	44.20	6.66	29.494	4.326	123.4 ± 2.8
1080	43.86	5.84	28.005	4.282	122.2 ± 3.1
1130	37.05	7.19	26.256	4.357	124.2 ± 2.5
1180	30.36	9.73	22.421	4.594	130.8 ± 1.9
1230	33.68	8.76	23.966	4.926	139.8 ± 2.2
1280	43.95	6.15	30.613	5.399	152.7 ± 3.1
1350	60.52	6.34	33.817	5.420	153.3 ± 4.1
Fuse	52.97	5.63	33.673	5.680	160.3 ± 3.2
					Total age = 132.8 ± 0.8

Notes: The ages are calculated using the decay constants recommended by Steiger and Jäger (1977). Correction factors for interfering isotopes produced by neutron irradiation in the McMaster reactor are (³⁶Ar/³⁷Ar)_{Ca} = 2.54 × 10⁻⁴, (³⁹Ar/³⁷Ar)_{Ca} = 6.51 × 10⁻⁴, and (⁴⁰Ar/³⁹Ar)_K = 2.87 × 10⁻²; atm = atmospheric, ⁴⁰Ar* = radiogenic ⁴⁰Ar. Ca and K are produced by Ca-neutron and K-neutron interferences, respectively.

excess argon are probably disturbed at low temperature by the additional degassing of young alteration phases.

The larger error bars obtained on the apparent ages of sample 85R18-23 are due to a lower K content (but similar Ca content), resulting in a higher relative contribution of Ca-derived interference isotopes and in atmospheric argon contamination.

The determination of an unambiguous, geologically meaningful age from these preliminary data is difficult because of the relative im-

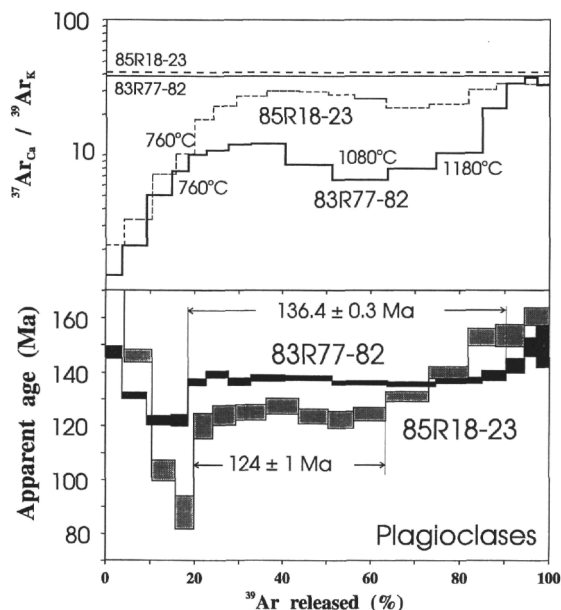


Figure 3. ⁴⁰Ar/³⁹Ar ages and (³⁷Ar_{Ca}/³⁹Ar_K) ratio spectra of plagioclase 83R77-82 and 85R18-23. The apparent age error bar for each temperature step is at the 1σ level. The composition of the plagioclases measured by the microprobe is shown on the ³⁷Ar_{Ca}/³⁹Ar_K spectrum: the Ca/K ratio measured with the microprobe has been converted in ³⁷Ar_{Ca}/³⁹Ar_K ratio by the relationship (K/Ca) = 0.539 × (³⁹Ar_K/³⁷Ar_{Ca}).

portance of secondary phases in the K-poor plagioclase. The questions we have to resolve are: (1) are the weighted mean ages (given in Fig. 3) calculated on the flat regions at intermediate temperatures geologically significant, and (2) how can we explain the difference between these two "plateau ages." We notice that despite a distinctly different initial grain size, these two rocks were originally similar and suffered the same tectono-metamorphic evolution. Moreover, they are only 16m distant, and therefore the two analyzed plagioclases should have recorded the same geological history.

The apparent ages of the flat region of the sample 83R77-82, ranging from 134.5 ± 0.8 to 138.8 ± 1.2 m.y., do not define a ⁴⁰Ar/³⁹Ar plateau age (which is the usual validity criterion for accepting a geologically significant age) because these extreme apparent ages are not concordant (even at the 2σ level) with the weighted mean age of 136.4 ± 0.3 Ma. The apparent ages are clearly correlated with the

$^{37}\text{Ar}_{\text{Ca}}/^{39}\text{Ar}_{\text{K}}$ ratios, indicating a probable higher contribution of younger K-rich secondary phases near 1100°C (as shown by Sebai et al., 1991, on altered plagioclases). The $^{36}\text{Ar}/^{40}\text{Ar}$ vs. $^{39}\text{Ar}/^{40}\text{Ar}$ correlation diagram on steps 820°-1350°C (not given) displays an age of 133.9 ± 0.7 Ma (Mean Square Weighted Deviation = 1.6, initial $^{40}\text{Ar}/^{36}\text{Ar}$ ratio = 318 ± 6).

Figure 4 reports the measured intensities of the isotopes $^{40}\text{Ar}^*$, $^{39}\text{Ar}_{\text{K}}$, and $^{37}\text{Ar}_{\text{Ca}}$ per °C, vs. temperature. We observed one main and wide degassing peak of $^{40}\text{Ar}^*$ and $^{39}\text{Ar}_{\text{K}}$ in Sample 83R77-82, whereas these isotopes were released in two temperature domains (two peaks) for sample 85R18-23. The $^{37}\text{Ar}_{\text{Ca}}$ is degassing in two peaks in both cases. The two "plateau-ages" were defined in the same temperature domain, and correspond to the first degassing peak of $^{40}\text{Ar}^*$, $^{39}\text{Ar}_{\text{K}}$, and $^{37}\text{Ar}_{\text{Ca}}$ for sample 85R18-23. The increasing high-temperature apparent ages displayed by sample 85R18-23 correspond to the second degassing peak of the three isotopes. Because the temperature of each step and the weight of analyzed samples were equivalent for the two experiments, we can quantitatively compare the degassing curves. The similarity of $^{37}\text{Ar}_{\text{Ca}}$ and the difference between both $^{40}\text{Ar}^*$ and $^{39}\text{Ar}_{\text{K}}$ degassing curves for the two samples clearly show that the two peaks of $^{37}\text{Ar}_{\text{Ca}}$ (both samples), and of $^{39}\text{Ar}_{\text{K}}$ and $^{40}\text{Ar}^*$ (sample 85R18-23) correspond to the degassing of "pure" plagioclase, whereas the single peaks of $^{39}\text{Ar}_{\text{K}}$ and $^{40}\text{Ar}^*$ (sample 83R77-82) correspond to a mixture of "pure" plagioclase and secondary phases included in the plagioclase.

When we compare the Ca/K ratio deduced from the $^{37}\text{Ar}_{\text{Ca}}/^{39}\text{Ar}_{\text{K}}$ ratio (by the relationship $[\text{K}/\text{Ca}] = 0.539 \times [^{39}\text{Ar}_{\text{K}}/^{37}\text{Ar}_{\text{Ca}}]$) with the microprobe results, we observe (Fig. 3) that the Ca/K ratio of the analyzed plagioclase 85R18-23 (at intermediate and high temperatures) almost corresponds to the composition of the plagioclase measured by the microprobe (the mean values were calculated from a more extensive data set than in Table 1), whereas the Ca/K ratio given by the plagioclase 83R77-82 is much lower. The combination of this observation with the interpretation of the degassing curves previously discussed clearly shows that the "plateau" segment of Sample 83R77-82 corresponds to the degassing of (1) the plagioclase itself and (2) secondary K-rich phases. Therefore, the validity of such a "plateau-age" must be viewed with caution. Nevertheless, we notice that on this "plateau" segment, the significant variation of the $^{37}\text{Ar}_{\text{Ca}}/^{39}\text{Ar}_{\text{K}}$ ratio (by a factor of 3) due to a strong and variable contribution of secondary K-rich phases produces maximum variations of apparent ages of about 3% only. This probably indicates that these secondary phases are not much younger than the closure time of the plagioclase.

The apparent ages of the flat region of sample 85R18-23 range from 119.8 to 127.2 m.y., corresponding to 44% of the total ^{39}Ar released (such a fraction is much too small to consider this flat region as a plateau-age), with error bars on the order of $\pm 2.3\%$ - 3.5% . The apparent age variations at low temperature (from 180 to 88 m.y.) and at high temperature (from 124 to 160 m.y.) are greater than for Sample 83R77-82. Both the $^{37}\text{Ar}_{\text{Ca}}/^{39}\text{Ar}_{\text{K}}$ ratio spectrum and the degassing curves in Fig. 4 show that this "plateau" section corresponds to the degassing of plagioclase less contaminated by K-rich secondary phases. The greater variation in apparent ages of this sample (on the whole age-spectrum) is probably a consequence of a relatively greater effect of alteration processes and excess argon on a K-poor sample. Albitization of the plagioclases in this rock is clearly observed in thin section and detected by the microprobe analyses (Table 1), although sericite was not seen in these plagioclases. If this alteration is significantly younger than the K/Ar closure time of the plagioclase, its effect on the apparent ages is higher for a nearly pure plagioclase (poor in K) (85R18-23) than for a similar plagioclase (83R77-82) contaminated by a K-rich phase (sericite) nearly contemporaneous with the K/Ar closure of the mineral. If this model is correct, we are in a peculiar situation where a K-rich contaminated plagioclase gives a more reliable age than a relatively purer (with regard to K content) plagioclase.

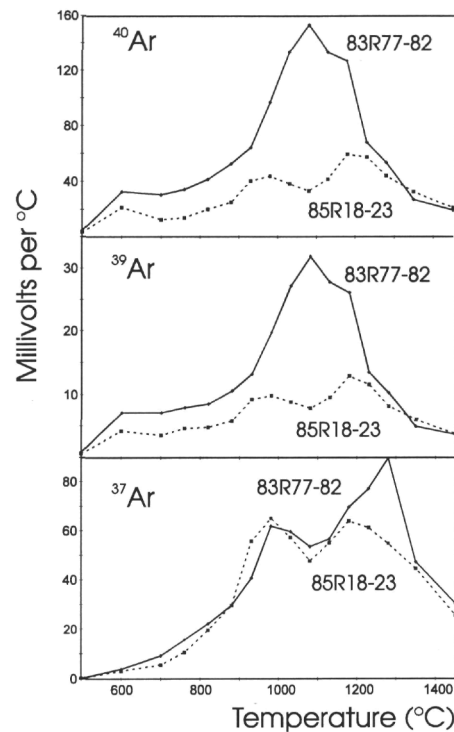


Figure 4. Degassing of individual isotopes $^{40}\text{Ar}^*$, $^{39}\text{Ar}_{\text{K}}$, and $^{37}\text{Ar}_{\text{Ca}}$ in millivolt per degree Celsius, vs. temperature, for plagioclases 83R77-82 (solid line) and 85R18-23 (dashed line) (1 millivolt = 7×10^{13} cm³ STP). Because similar quantities of sample were analyzed, the relative volumes of gas released can be compared.

INTERPRETATION OF DATA AND CONCLUSIONS

According to Cornen et al. (chapter 26, this volume), the composition of the Site 900 gabbros is close to that of basalts, dolerites, and gabbros from the OCT of the adjacent Galicia Margin, which was probably formed at the end of the Mesozoic continental rifting by interaction between a MORE source and enriched continental mantle (Kornprobst et al., 1988; Schärer et al., 1995). For this reason, and also because no similar rocks of Hercynian affinity have been identified close to Site 900 either on the western Iberia Margin or on land, these gabbros are more likely related to the Mesozoic syn-rift event rather than to the mobilization of Hercynian basement during margin formation, or to true oceanic accretion in the Atlantic domain.

The main petro-structural constraints on the evolution of the Site 900 gabbros, previously discussed in detail, are the following. The oldest recognizable tectonic event is a dynamic recrystallization during a shear deformation which developed the foliation and porphyroclastic or granuloblastic texture of these rocks. This deformation is intense and homogeneously distributed over the whole drilled section. The phase composition (Na- and Al-rich pyroxenes + spinel) suggests high-pressure conditions of dynamic recrystallization (0.4 GPa; Cornen et al., chapter 26, this volume). This ductile deformation was followed by a static retrograde metamorphism under greenschist facies conditions. A late low-temperature deformation event, aided by the circulation of hydrothermal fluids, led to fractures filled with chlorite, fibrous amphibole, epidote, zoisite, and later calcite. This deformation, which is unevenly distributed throughout the cores, locally brecciated the rocks and formed late shear zones in some intervals of high chlorite-vein density. The two investigated samples belong to zones preserved from this late deformation.

This evolution is comparable and compatible with that of the peridotites drilled at Site 897. These mantle rocks underwent a high-temperature shear deformation, a limited partial melting, and a subsolidus reequilibration in the plagioclase-stability field, followed by a mylonitic shear deformation. This high-temperature evolution is overprinted by extensive deformation under sub-surface conditions, aided by hydrothermal fluid circulation, during and after the serpentinization of the rocks. This evolution is compatible with uplift beneath the rift zone (Beslier et al., this volume; Cornen et al., chapter 26, this volume).

On the adjacent northern Galicia Margin (Fig. 1), the mantle rocks drilled at the OCT underwent a similar evolution during their uplift beneath the rift zone (Girardeau et al., 1988; Kornprobst et al., 1988). The partial melting of the rocks is expressed in particular by the occurrence of syn-kinematic dioritic dikes, and by a horizon at the top of the mantle of sheared chlorite-bearing schists derived from former gabbros (*Galinaute* diving sites 9-10; Fig. 1). Geochronological constraints show that emplacement and cooling of these mafic rocks occurred over a short time period (around 3.4 Ma) during the last stages of continental rifting (Féraud et al., 1988; Boillot et al., 1989; Schärer et al., 1995).

Although extra $^{40}\text{Ar}/^{39}\text{Ar}$ analyses (in progress) are needed to correctly interpret the data presented here, and for reasons previously given, we may consider the weighted mean age of 136.4 ± 0.3 m.y. as a reasonable estimate of the closure time of the plagioclase (the closure temperature of plagioclase is estimated in the range 200°-250°C; McDougall and Harrison, 1988). This age corresponds to the K/Ar closure of these minerals at the end of the retrograde metamorphic event recorded by the gabbros. Moreover, this age is about 11 m.y. older than the late Barremian age of the oldest sediments recovered in the OCT (Kent and Gradstein, 1986), on the peridotitic basement at Site 897, which clearly postdate the continental breakup of the margin.

Considering the nature and the evolution of the basement in the OCT of the Iberia Abyssal Plain, and by analogy with the adjacent deep Galicia Margin, this age is consistent with emplacement of these rocks in the thinned continental lithosphere during the last stages of continental rifting. The high-pressure conditions of dynamic recrystallization supported by their mineralogical composition suggest that, before the static metamorphism, the gabbros were ductilely sheared at mid-crustal depths. They may represent either (1) gabbros underplated at the base of the thinned continental crust (according to this hypothesis, the shear may have developed in a normal shear zone having a synthetic relationship to the normal faults delimiting the upper crustal blocks during the formation of the margin); or (2) gabbros trapped as a thick sill in the upper part of the mantle and sheared during the mylonitization of the surrounding peridotite.

The age of 136.4 ± 0.3 m.y. is intermediate between the 122 ± 0.3 Ma $^{40}\text{Ar}/^{39}\text{Ar}$ plateau-age measured by Féraud et al. (1988) on a dioritic dike intruding ultramafic rocks of the Galicia Margin (dive sites 9-10, Fig. 1), and 142.1 ± 0.5 Ma and 143.9 ± 0.7 m.y. $^{40}\text{Ar}/^{39}\text{Ar}$ plateau-ages measured on the amphiboles from gabbros of Goringe Bank, to the south (Féraud et al., 1986). These three geochronological data are consistent with a northward propagation of the Atlantic Ocean opening as suggested by Klitgord and Schouten (1986).

Hence, although there is no direct evidence to demonstrate that the Site 900 gabbros formed during the Mesozoic rifting of the margin, petrological characteristics, their tectono-metamorphic evolution, and dating of the latest retrograde metamorphism that they underwent (at the end of the continental rifting) strongly suggest that they formed during the rifting.

ACKNOWLEDGMENTS

We are indebted to M. Bohn, R. Derval and M. Manetti for their technical skills. This work was supported by the INSU/CNRS Grant Océanoscope.

REFERENCES

- Beslier, M.-O., Ask, M., and Boillot, G., 1993. Ocean-continent boundary in the Iberia Abyssal Plain from multichannel seismic data. *Tectonophysics*, 218:383-393.
- Bloomer, S.H., Natland, J.H., and Fisher, R.L., 1989. Mineral relationships in gabbroic rocks from fracture zones of Indian Ocean ridges: evidence for extensive fractionation, parental diversity, and boundary-layer recrystallization. In Saunders, A.D., and Norry, M.J. (Eds.), *Magmatism in the Oceanic Basins*. Geol. Soc. Spec. Publ. London, 42:107-124.
- Boillot, G., Féraud, G., Reccq, M., and Girardeau, J., 1989. "Undercrusting" by serpentine beneath rifted margins: the example of the west Galicia Margin (Spain). *Nature*, 341:523-525.
- Boillot, G., Girardeau, J., and Kornprobst, J., 1988. Rifting of the Galicia Margin: crustal thinning and emplacement of mantle rocks on the seafloor. In Boillot, G., Winterer, E.L., et al., *Proc. ODP, Sci. Results*, 103: College Station, TX (Ocean Drilling Program), 741-756.
- Bonatti, E., and Seyler, M., 1987. Crustal underplating and evolution in the Red Sea rift; uplifted gabbro/gneiss crustal complexes on Zabargad and Brothers islands. *J. Geophys. Res.*, 92:12803-12821.
- Féraud, G., Girardeau, J., Beslier, M.O., and Boillot, G., 1988. Datation $^{39}\text{Ar}/^{40}\text{Ar}$ de la mise en place des péridotites bordant la marge de la Galice (Espagne). *C. R. Acad. Sci. Ser.*, 2, 307:49-55.
- Féraud, G., York, D., Mével, C., Cornen, G., Hall, C.M., and Auzende, J.M., 1986. Additional $^{40}\text{Ar}/^{39}\text{Ar}$ dating of the basement and the alkaline volcanism of the Goringe Bank (Atlantic Ocean). *Earth Planet. Sci. Lett.*, 79:255-269.
- Girardeau, J., Evans, C.A., and Beslier, M.-O., 1988. Structural analysis of plagioclase-bearing peridotites emplaced at the end of continental rifting: Hole 637A, ODP leg 103 on the Galicia Margin. In Boillot, G., Winterer, E.L., et al., *Proc. ODP, Sci. Results*, 103: College Station, TX (Ocean Drilling Program), 209-223.
- Helmstaedt, H., and Allen, J.M., 1977. Metagabbro from DSDP Hole 334: an example of high temperature deformation and recrystallization near the Mid-Atlantic ridge. *Can. J. Earth Sci.*, 14:886-898.
- Honnorez, J., Mével, C., and Montigny, R., 1984. Geotectonic significance of gneissic amphibolites from the Vema fracture zone, equatorial Mid-Atlantic Ridge. *J. Geophys. Res.*, 89:11379-11400.
- Kent, D.V., Gradstein, F.M., 1986. A Jurassic to recent chronology. In Vogt, P.R., and Tucholke, B.E. (Eds.), *The Geology of North America* (Vol. M): *The Western North Atlantic Region*. Geol. Soc. Am., 45-50.
- Klitgord, K.D., and Schouten, H., 1986. Plate kinematics of the central Atlantic. In Vogt, P.R., and Tucholke, B.E. (Eds.), *The Geology of North America* (Vol. M): *The Western North Atlantic Region*. Geol. Soc. Am., 351-378.
- Kornprobst, J., Vidal, P., and Malod, J., 1988. Les basaltes de la Marge de Galice (NO de la Péninsule Ibérique): hétérogénéité des spectres de terres rares à la transition continent/océan. Données géochimiques préliminaires. *C. R. Acad. Sci. Ser.*, 2, 306:1359-1364.
- Lallemand, S., Mazé, J.P., Monti, S. and Sibuet, J.C., 1985. Présentation d'une carte bathymétrique de l'Atlantique Nord-Est. *C. R. Acad. Sci. Ser.*, 2, 300:145-149.
- McDougall, I., and Harrison, T.M., 1988. *Geochronology and Thermochronology by the $^{40}\text{Ar}/^{39}\text{Ar}$ Method*: New York (Oxford Univ. Press).
- Mercier, J.-C.C., Anderson, D.A., Carter, N., 1977. Stress in the lithosphere: inference from steady-state flow of rocks. *Pure Appl. Geophys.*, 115:129-226.
- Sawyer, D.S., Whitmarsh, R.B., Klaus, A., et al., 1994. *Proc. ODP, Init. Repts.*, 149: College Station, TX (Ocean Drilling Program).
- Schärer, U., Kornprobst, J., Beslier, M.O., Boillot, G., and Girardeau, J., 1995. Gabbro and related rock emplacement beneath rifting continental

- crust: U-Pb geochronological and geochemical constraints for the Galicia passive margin (Spain). *Earth Planet. Sci. Lett.*, 130:187-200.
- Sebai, A., Féraud, G., Bertrand, H., and Hanes, J., 1991. $^{40}\text{Ar}/^{39}\text{Ar}$ dating and geochemistry of tholeiitic magmatism related to the early opening of the Central Atlantic rift. *Earth Planet. Sci. Lett.*, 104:455-472.
- Shipboard Scientific Party, 1993. ODP drills the West Iberia rifted margin. *Eos*, 74:454-455.
- Steiger, R.H., and Jäger, E., 1977. Subcommittee on geochronology: convention on the use of decay constants in geo- and cosmochemistry. *Earth Planet. Sci. Lett.*, 36:359-362.
- Whitmarsh, R.B., Pinheiro, L.M., Miles, P.R., Recq, M., and Sibuet, J.C., 1993. Thin crust at the western Iberia ocean-continent transition and ophiolites. *Tectonics*, 12:1230-1239.

Date of initial receipt: 27 February 1995

Date of acceptance: 19 July 1995

Ms 149SR-224